Results from One- and Two- Phase Fluid Flow Calculations within the Preliminary Safety Analysis of the Gorleben Site – 13310

Ingo Kock, Jürgen Larue, Heidi Fischer, Gerd Frieling, Martin Navarro and Holger Seher
Department of Final Disposal, GRS mbH, Schwertnergasse 1, 50667 Cologne – Germany,
Ingo.Kock@grs.de

ABSTRACT

Rock salt is one of the possible host rock formations for the disposal of high-level radioactive wastes in Germany. The Preliminary Safety Analysis of the Gorleben Site (Vorläufige Sicherheitsanalyse Gorleben, VSG) evaluates the long-term safety of a hypothetical repository in the salt dome of Gorleben, Germany. A mature repository concept and detailed knowledge of the site allowed a detailed process analysis within the project by numerical modeling of single-phase and two-phase flow. The possibility of liquid transport from the shafts to the emplacement drifts is one objective of the present study. Also, the implications of brine inflow on radionuclide transport and gas generation are investigated. Pressure build-up due to rock convergence and gas generation, release of volatile radionuclides from the waste and pressure-driven contaminant transport were considered, too. The study confirms that the compaction behavior of salt grit backfill is one of the most relevant factors for the hydrodynamic evolution of the repository and the transport of contaminants. Due to the interaction between compaction, saturation and pore pressure, complex flow patterns evolve. Emplacement drifts serve as gas sinks or sources at different times. In most calculation cases, the backfill reaches its final porosity after a few hundred years. The repository is then sealed and radionuclides can only be transported by diffusion in the liquid phase. Estimates for the final porosity of compacted backfill range between 0 % and 2 %. The exact properties of the backfill regarding single- and two-phase flow are not well known for this porosity range. The study highlights that this uncertainty has a profound impact on flow and transport processes over long time-scales. Therefore, more research is needed to characterize the properties of crushed salt grit at low porosities or to reduce the adverse effects of possible higher porosities by repository optimization.

INTRODUCTION

In Germany, the Gorleben salt dome has been discussed as a possible site for a repository for heat-generating radioactive waste since the 1970s. The project *Preliminary Safety Analysis for the Gorleben Site* (Vorläufige Sicherheitsanalyse Gorleben, VSG) provides a comprehensive safety analysis for the site with a focus on long-term safety (see accompanying paper [1]). A main goal of the project is to identify the need for future R&D work and site investigations at the Gorleben site. It is important to note that the safety demonstration provided by the VSG project is not part of a licensing procedure, which is required by the German Atomic Energy Act.

The Preliminary Safety Analysis implements the German safety requirements for the final disposal of heat-generating radioactive wastes of 2010 [2]. These requirements call for the provision of a so called ***containment providing rock zone*** **(CPRZ)**, which envelopes the repository mine and assures safe containment of radionuclides. By using numerical models it has to be shown that the integrity of the geological barrier is maintained and no inadmissible release of radionuclides from the CPRZ takes place. This requires thorough understanding of the processes acting in the repository. Although undisturbed rock salt is almost impermeable and its mechanical behavior is well known, processes in the repository appear to be complex. A main reason for this is the intense interaction between fluid flow and rock convergence, which drives the compaction of the crushed salt backfill – the geotechnical long-term barrier. This coupled process is complicated by its dependency on temperature and backfill moisture. Back fill compaction as well as gas generation, the latter limited by the availability of water, increase pore pressure. This again drives the transport of brine, gas and contaminants. If gas pressure rises above certain

thresholds gas infiltration into the rock will occur. Elevated gas pressure may violate the integrity of the geological or engineered/technical barrier if there is a sufficient supply of gas.

Since brine and gas flow may cover large distances the entire repository has to be captured in the models. Numerical models for the repository that describe the mentioned processes including two-phase flow had not been available in the past. In the VSG project, such a model was applied for the first time. This model is a modification of the multi-phase flow code TOUGH2 (**T**ransp**o**rt of **U**nsaturated **G**roundwater and **H**eat) of the Lawrence Berkeley Laboratory, in which additional processes relevant to repositories in rock salt have been included. The single-phase flow code MARNIE (which is an acronym for "**M**odell zur **A**usbreitung von **R**adio**N**ukliden **I**m **E**ndlagerbergwerk" meaning "model for the release of radionuclides in a final repository"), which has been developed by GRS, was applied to calculate the mobilization and advective - diffusive transport in brine of a large number of radionuclides with radioactive decay and decay-chains.

The repository, the expected processes and the applied numerical models are described below. Results are shown to illustrate pressure build-up, fluid and radionuclide transport in the repository.

DESCRIPTION

Repository Concept

During the project, several alternative repository concepts were developed [3, 4]. The concept described here is the so called *B1* concept. In this concept, high active and heat-generating waste is emplaced in horizontal drifts. There are two almost parallel main drifts extending roughly in E-W direction (the principal repository layout is displayed in Fig. 1). Twelve emplacement fields with associated cross drifts are aligned between the two main drifts. Emplacement fields were numbered consecutively from farthest (East 1) to nearest (East 12) with respect to the shafts. Each emplacement field consists of 7 to 16 emplacement drifts. The precise number of drifts depends on the available space and on drift spacing, which is determined by the greatest permissible temperature in the host rock of 200 °C.

POLLUX®, CASTOR® and cast iron containers are intended to accommodate the wastes. The wastes originate from nuclear research reactors, reprocessing plants, and nuclear power plants (pressure-water, boiling-water and water-water reactors). Most of the wastes show a significant heat production. Additionally, 2620 cast iron containers filled with structural components from dismantling nuclear fuel will be emplaced.

Backfill made out of crushed salt is the main technical long-term barrier. The backfill compacts due to the convergence of the surrounding rock thereby sealing the backfilled drifts. The estimate for the minimum porosity that the backfill can achieve is 1 % ± 1 %. Since moisture accelerates the compaction of backfill, slightly moistened backfill is emplaced in the main drifts (0.6 wt. % moisture).

Dry backfill (max. 0.02 wt.-% moisture) is used for the cross drifts and emplacement fields. The elevated temperature in these areas accelerates rock convergence significantly so that a complete compaction of the dry backfill is achieved after a few decades [5].

Compaction in backfilled drifts takes time so that quick-acting seals are emplaced in the access drifts [6]. These drift seals have an average permeability of $5 \cdot 10^{-17}$ m², which already takes the excavation damaged zone (EDZ) into account.

The shaft seals are complex structured columns of approx. 500 m height [6]. They contain seals of Sorel-concrete (permeability: $5 \cdot 10^{-17}$ m²), salt-concrete (permeability: $7 \cdot 10^{-19}$ m²) and bentonite (permeability:

$7.8 \cdot 10^{-17}$ to $1 \cdot 10^{-17}$ m²) as well as one long-term barrier consisting of pre-compacted salt grit (10 % porosity). Furthermore, a reservoir for fluids consisting of highly porous gravel was incorporated into the shaft sealing structure.

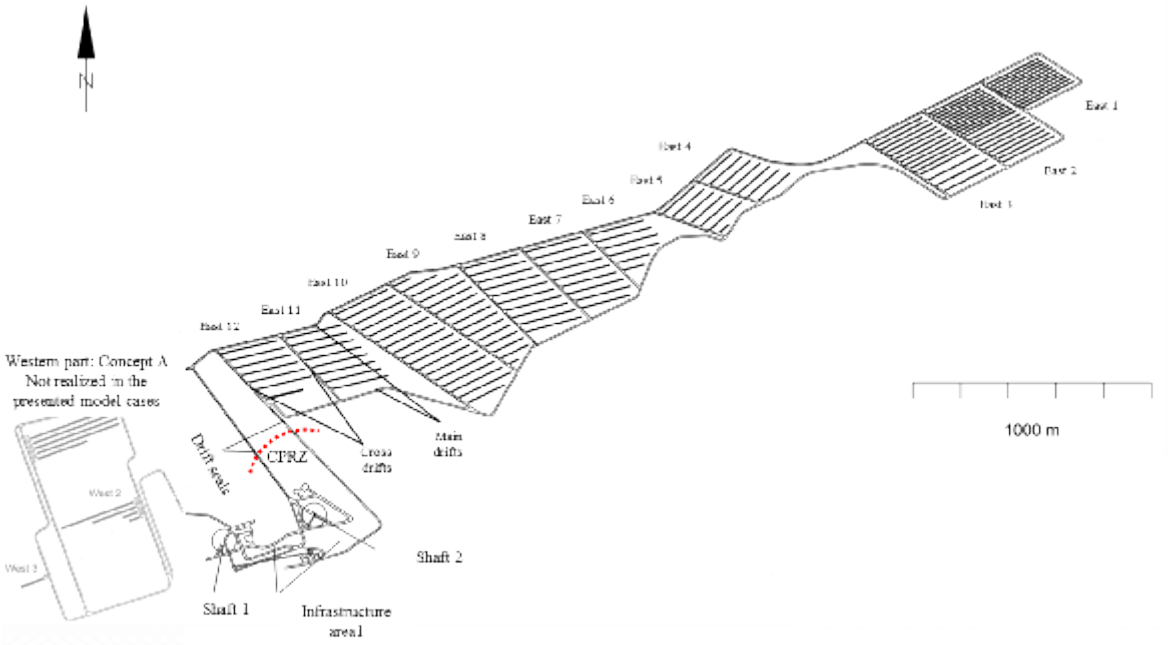

Fig. 1. Repository layout. The concept *B1* corresponds to the eastern part. The western part is not realized in the presented model cases (modified from [3, 4]). CPRZ through both seals is shown in red.

The infrastructure area (workshops, etc.) around the two main shafts is filled with non-compactable basalt gravel and brucite with a porosity of 38 %. The volume of these cavities amounts to 440,000 m³. Accordingly, 167,200 m³ of pore space is available for storage of brine or gas. If a shaft seal fails, the storage provided by the infrastructure area will impede the entry of brine into the main drifts until they are sealed by the compacting backfill. Further on, contaminated gases that might escape from the repository will be retained in the storage, which avoids concentration peaks at the shaft seals.

For all seals, separate proofs e.g. of long-term stability (50,000 years expected lifetime) were part of the project [7].

Numerical Tools

Two-phase flow was simulated using the code TOUGH2. This code was developed by Lawrence Berkeley Laboratory, USA, for the simulation of 3-dimensional multi-phase, heat and radionuclide transport in porous media [8]. A generalized Darcy-law is used to simulate density driven flow. By means of equation-of-state (EOS) modules different phases, components and thermo-dynamical processes can be simulated. The modules EOS7 and EOS7R were used in this study because of their ability to consider brine.

Several new processes were implemented into the code to cover the processes that are relevant in a salt rock repository. Among these are

- the compaction of backfill as a time, pressure, and temperature dependent process

- the generation of gas taking into account the availability of water for metal corrosion
- increasing permeability of seals due to degradation
- gas infiltration into the host rock if pore pressure exceed the minimal principal stress
- a prescribed variable temperature field

Prescription of a variable temperature field was necessary because no heat-transport was calculated. The reason for this is that only the mining caverns and no host rock were considered in model grid in order to save computation time.

It is assumed that there is an infiltration of gas into the host rock if the gas pressure exceeds the lithostatic pressure of 18.8 MPa. This process is simulated by reducing the pressure to the lithostatic pressure and calculating the corresponding gas loss.

The code MARNIE [9] is a transient, coupled single-phase transport code for networks of one-dimensional structures, such as drifts, shafts and caverns. The code was developed by GRS in the late 1980s for the application to repositories in rock salt. The code was further developed in the following years.

MARNIE calculates transport of brine and brine contaminants. The code simulates advective - diffusive transport including hydrodynamic dispersion. MARNIE also considers convergence of cavities with corresponding compaction of backfill, container failure, mobilization and decay of radionuclides, solubility limits, sorption, and temperature impacts. The number of radionuclides is not limited. Radionuclides can be part of an unlimited number of decay-chains.

Although MARNIE considers the effect of gas pressure on brine flow, the code does not simulate the transport of gas or transport of contaminants in the gas phase. This is because MARNIE was originally designed for the case of repository flooding where gases can escape easily.

MARNIE distinguishes between an inflow (flooding) phase and a long-term phase. In the inflow phase only brine flow, rock convergence and decay of radionuclides in the containers are calculated. In the long-term phase the entire repository is saturated and radionuclide transport may take place.

Modeling Compaction

Convergence of the host rock due to salt creep and subsequent compaction of the salt grit backfill are important driving forces for fluid transport and pressure evolution in the repository. In our models, backfill compaction is considered using a simplified approach which minimizes calculation time.

The compaction rate $\dot{k}$ is calculated as a pressure and porosity dependent function,

$$\dot{k} = \dot{k}_{ref} \cdot f_{cal} \cdot f_P \cdot f_\phi \qquad \text{(Eq. 1)}$$

where $\dot{k}_{ref}$ is a reference compaction rate for a reference depth, f_{cal} a calibration factor, f_P a pore pressure dependent term, and f_ϕ a term describing the mechanical support of the backfill at porosity ϕ. Further information on this approach can be found in [9, 10].

Eq. 1 does not describe the strong temperature dependency of the compaction rate. The reason for this is the significant uncertainty regarding temperature evolution. Eq. 1 was therefore calibrated using thermo-

mechanical calculations that were performed with Code_Bright® in the VSG project [7, 11]. For the calibration, the compaction behavior (i.e. time to compact to 1 % or 2 % porosity; 5 % was only used for calibration) was divided into five categories of temperature and moisture (Table I). Emplacement drifts for spent fuel, for instance, fall into the category of dry and hot salt grit. In view of a more conservative approach on salt grit compaction, longer compaction times were also considered in the models. In general, salt grit was allowed to compact to a porosity of 1 % but some calculations also consider a higher limit of 2 %.

Table I. Categories of compaction behavior for salt grit

	Compaction time* [a]						Location
Compaction	fast			slow			
Category	to 5 %	to 2 %	to 1 %	to 5 %	to 2 %	to 1 %	
Dry, hot	10	25	40	50	120	200	Emplacement drifts, fields 3 to 12
Dry, warm	80	200	300	200	490	800	Cross drifts, fields 3 to 12
Dry, cold	800	1925	3200	1000	2400	4000	Emplacement drifts, fields 1 to 2
Moist, warm	50	70	100	100	140	300	Main drifts between fields 3 to 12
Moist, cold	80	115	140	200	280	370	Main drifts between fields 1 to 2 and to drift seal

*5 % porosity was used only for curve fitting, since final porosity values as end-points of the curve do not work for curve fitting

As porosity ϕ decreases, backfill permeability K is reduced. Compilation of available data sets (in [12]) allow for an empirically derived relation,

$$K = A \cdot \phi^n \qquad \text{(Eq. 2)}$$

where A and n are material parameters. For different porosity ranges, A and n were chosen as displayed in Table II and determined by curve fitting [13, 14]. Accordingly, for a lower porosity limit of 1 % the lowest permeability that can be achieved is $3 \cdot 10^{-20}$ m². The non-vanishing permeability reflects the uncertainty regarding the connectivity of pores. However, it is expected that no interconnected pore space is available at 1 % porosity.

Table II. Parameter range for Eq. 2

Porosity range	A [m²]	n
$0.1 < \phi < 1$	$2 \cdot 10^{-9}$	4.8
$0.05 < \phi < 0.1$	$6.7 \cdot 10^{-5}$	9.32
$0.01 < \phi < 0.05$	$4.99 \cdot 10^{-11}$	4.61

Modeling Gas Generation

A second driving force for fluid flow and pressure build-up is the generation of gas by corrosion. Although moisture content in the salt grit is supposed to be very low in the emplacement drifts (0.02 wt. %) the large volume of backfill still leads to approx. 34 kg of moisture (water) per Pollux® container, which could be available for corrosion. Other processes such as microbiological degradation or thermochemical sulfate reduction may increase water content in the emplacement drifts but are hard to

quantify. Therefore, the water available for corrosion was set to the water content of the backfill plus the water content from the wastes.

It is possible that various containers include residual water e.g. from waste conditioning [15, 16]. Realistic estimates regarding the Pollux®-containers lead to approx. 60 g of moisture per container. Very pessimistic guesses (i.e. every fuel rod damaged, with maximum water content, damage undetected and then enclosed in the containers) yielded 18 kg water per container. For the complete water content of the emplacement fields available for corrosion (backfill + container) see Table III.

Consequences of both variants were calculated. Since corrosion rates depend on the chemical conditions and on the available water content rates between 0.04 and 100 µm/a were considered [17].

Table III. Water content (locations are displayed in Fig. 3)

Location	Water content [kg] per container including salt grit moisture		Number of containers
	pessimistic estimate	realistic estimate	
Field East 1:	32.46	14.46	511
Field East 2:	55.87	53.47	906
Fields East 3 - 12:	55.62	37.68	2120
Southern emplacement drift of Field East 12:	2.23	2.23	2620

Source Term

The radioactive inventory for all waste forms to be disposed of in the repository is derived for fission and activation products as wells as from the Thorium, Neptunium, Uranium and Actinium decay chains [16]. Radionuclides with a half live < 20 years were excluded. The release of an Instant Release Fraction (IRF) of radionuclides was considered for high soluble nuclides in both, the liquid and gas phase. Solubility limits for all nuclides in the inventory were determined for a Mg saturated solution by [18], since the brine composition will be Mg saturated due to the brucite deposit in the infrastructure area.

The transport of radionuclides in the gas phase was simulated for selected radionuclides of the IRF. Extremely volatile molecules (CO_2 or CH_4) containing C-14 were regarded as important for radionuclide transport. Conservatively, the entire C-14 content was supposed to be present in form of CH_4. Dissolution of CH_4 in the gas phase was calculated using a Henry coefficient of 0.0014 mol/l·atm [19]. A normalized amount of C-14 was used as a tracer so that concentrations or mass flow will be expressed as fractions of the initial amount per m³ or year in the following.

The CPRZ envelops the repository and must cut through the mine in at least one place. For the presented repository concept it is designated to run through both drift seals (Fig. 1). Therefore, for all calculations, transport of radionuclides is monitored for both drift seals.

Calculation Cases

The repository concept *B1,* as described above, was transferred into a 1D network for MARNIE (Fig. 2) and to a 3D grid for TOUGH2 (Fig. 3).

The model grid for MARNIE includes two shafts, two infrastructure areas at different depth and several emplacement fields in E-W direction (see Fig. 2). All elements in the repository are modeled with the

dimensions and volumes given in the repository concept. After an expected lifetime of 50,000 years the seals degrade which is simulated by multiplying the permeability by a factor of 10^3.

Several numerical cases have been calculated using the code MARNIE. Primarily the permeability of the shaft seals, the final porosity, reached by salt grit compaction, the rate of compaction (slow or fast, see Table I) are varied for each case.

Commencing with the disposal of the first canister in field East 1, the temperature evolution in the repository due to the heat generating waste is considered. Compaction of salt grit and permeability reduction are implemented according to above described approaches. MARNIE calculations are purely hydraulic, gas generation has not been taken into account, but gas pressure increase due to compaction of the enclosed air is allowed for. Radionuclide mobilization from different waste species is computed using the mathematical mobilization models given in [18, 20]. Compaction of the backfill and the decay of the inventory in an emplacement field begin, when the drifts are backfilled. The simulation time for all calculations is 10^6 years.

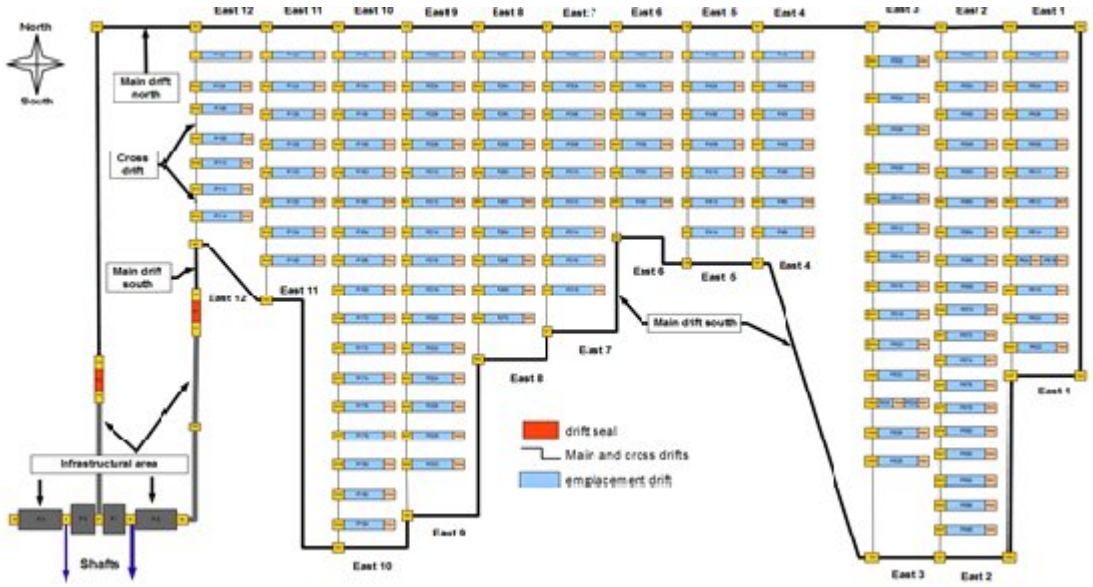

Fig. 2. MARNIE 1D network of the repository emplacement level (map view; schematic representation of the modeling grid).

For TOUGH2, some simplifications regarding the transfer from repository concept to 3D grid had to be made. Notably this includes the constraint to an orthogonal grid due to numerical reasons. In order to achieve volumetric consistency with the repository concept, drift height and width were adjusted. Note that drift lengths from the repository design had to be adjusted. Lengths of drifts were not increased in any case so that transport time is underestimated. Numerous calculation cases were considered during the project and only a few can be shown here. These cases focus on:

i) the evolution of maximum gas pressure in the repository (cases P),
ii) and the possible release of C-14 from the Initial Release Fraction (IRF) with respect to the waste from structural components in the southern drift of field East 12 (cases SC).

Some specifications for the model cases are shown in Table III.

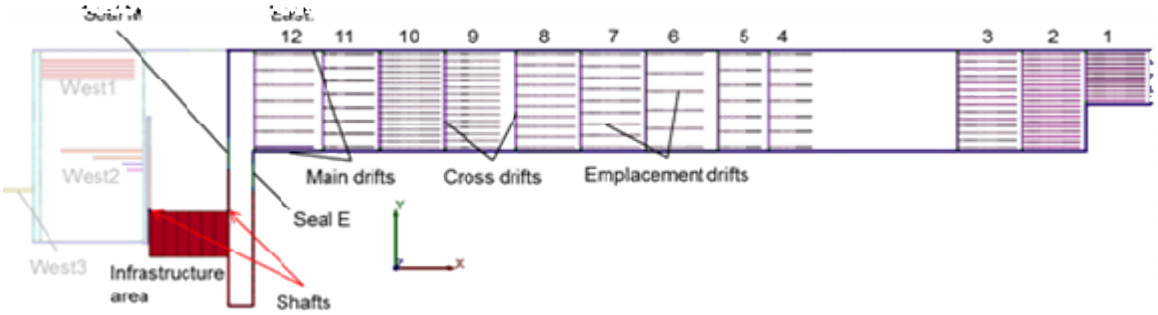

Fig. 3. Plan view of TOUGH2 repository layout for concept *B1* (intense colors) and *A* (light colors, no results documented here).

Table III. Features of selected TOUGH2 calculation cases

Case	Corrosion rate [µm/a]	Final porosity* [-]	Water content	Other conditions / remarks
P-1	0.04	0.01	initial conservative estimate	
P-2	0.1	0.01		
P-3	5.1	0.01		
P-4	15	0.01		
P-5	100	0.01		
P-6	0.1	0.02		
P-7	0.1	0.01	realistic estimate	
P-8	0.1	0.01	realistic estimate	container pore space available
SC-1	0.0	0.01	initial conservative estimate	C-14 release in southern drift of field East 12
SC-2	0.04			
SC-3	0.1			
SC-4	5.1			
SC-5	15			

* initial porosity in all cases was 0.38

Results of MARNIE Calculations

The calculations with MARNIE only consider the transport of radionuclides in the saturated liquid phase. Transport of radionuclides occurs if brine reaches the canisters in the emplacement drifts and mobilization from the waste matrix takes place. Advective brine transport is only modeled when the porosity of the compacted crushed salt backfill is > 1%. Therefore in numerical cases with a final porosity of 1 %, no inflow of brine was observed into the emplacement drifts. Assuming slow salt grit compaction, porosity in the main drifts reached 1 % after 700 years at the latest and even earlier for fast compaction. Postulating the expected lifetime of the shaft seals, filling of the infrastructure area started after 50,000 years. After this time all drifts of the repository had reached the final porosity of 1 %, therefore no advective brine inflow was possible. Assuming shaft failure directly after the closure of the repository, the infrastructure area was filled within 1,000 years. Shaft failure is modeled here by setting the permeability of the shaft sealing to 10^{-15} m^2. Even in this case no advective brine inflow into the emplacement drifts was observed, since the final porosity of 1 % was reached in the main drifts before the infrastructure area was filled.

Only in numerical cases with an assumed final porosity of 2 % the brine reached the emplacement fields. The results of one of these numerical cases will be discussed here. The following assumptions are postulated:

- Normal evolution of the shaft sealings (expected lifetime 50,000 years),
- Final porosity 2 % with a resulting permeability of $7{,}5 \cdot 10^{-19}$ m^2 and assumed advective flow
- Diffusion coefficient $1 \cdot 10^{-10}$ m^2/s (conservative assumption since the data base for salt grit at low porosities in insufficient)

In this case, the inflow phase into the repository began after the shaft seals reached their lifetime of 50,000 years. Subsequently, within less than 1,000 years, the infrastructure area at the repository level and the drift seals were saturated with brine. Shortly after that, the connecting main drift between the drift seal and the emplacement field East 12 (Fig. 2) was filled. Saturation of the first cross drift of emplacement field East 12 took another 1,000 years. Approximately 2,500 years after shaft failure the first emplacement drift (emplacement field East 12) had been saturated with brine. The subsequent emplacement drifts are saturated consecutively. Radionuclides are mobilized from the canisters as soon as the respective emplacement drift is filled.

Fig. 4 shows the saturation of the repository at the end of simulation time. After 10^6 years, all emplacement fields between field 12 and field 7 are completely saturated with brine, with emplacement field 6 only partially saturated. Full saturation for the main drifts can be observed as far as emplacement field 5. Due to the fact that several emplacement fields remained unsaturated and assuming atmospheric pressure in these fields, the inflow into the repository had not finished after 10^6 years. Further calculations show that the whole repository is saturated after approx. $3 \cdot 10^6$ years and the inflow stops. Until this time, the released radionuclides from the emplacement drifts are transported within the advective flow towards the unsaturated areas. The radionuclide transport towards the drift seals and the infrastructure area was driven only by diffusion.

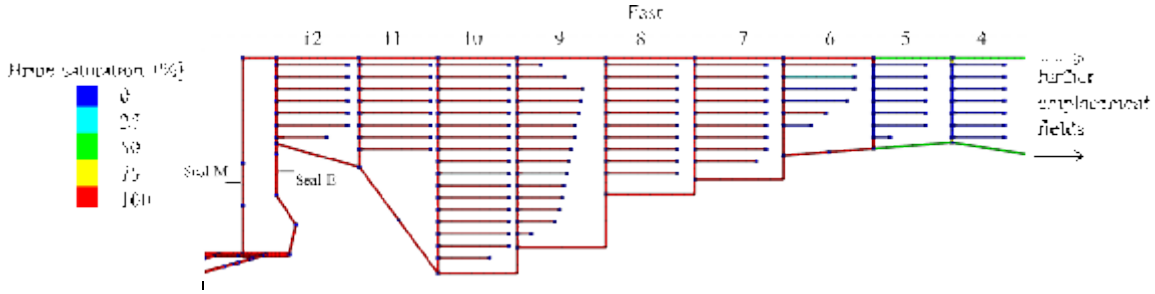

Fig. 4. Brine content of the presented case at the end of the calculations at approx. 10^6 years.

Fig. 5 shows the activity flow through the eastern drift seal next to emplacement field East 12 (Fig. 2) for some important radionuclides. The activity flow through the eastern drift seal (Seal E) was several orders of magnitude higher than the activity flow over the drift seal M. Because radionuclide transport to the drift seals is only driven by diffusion, the gradient of radionuclide concentration is very important for radionuclide transport. The saturated infrastructure area has a huge dilution capability due to its high pore volume (87.400 m^3 due to basalt grit backfill with 38% porosity), so that the amount of the net diffusive flow becomes higher near the infrastructure area. The transport path from emplacement field East 12 via the northern main drift to the drift seal M is much longer than via the southern main drift to the eastern drift seal E. Thus, only radionuclide release for the eastern seal (Seal E) is shown.

After approximately 70,000 years the activity flow of Ni-59 increased until 250,000 years (Fig. 5). Up to approximately 800,000 years this constituted the maximum. The subsequent decrease was mainly due to the radioactive decay of Ni-59 with a half-life of $7.5 \cdot 10^4$ years. After 800,000 years, higher activity was shown by Zr-93. Because of its higher half-life ($1.5 \cdot 10^6$ years) the activity flow did not decrease again but continued to rise. High activity flows are also observed for Tc-99 and Cl-36. Activity flow of Nb-94 also rose strongly at first but decreases equally strong because of its relative short half-life of 20,000 years. Activity flow of all other shown radionuclides increase over time also, but at a significantly lower level. Regarding the consequences for human safety, note that the activity flow is very small (max 10^{-5} Bq/a). The corresponding theoretical dose using an exposition model for liquids is negligible.

Regarding these results, note that some assumptions are very conservative with respect to the release of radionuclides. The possibility of advection and diffusion at a final porosity of 2 % in compacted salt grit has to be clarified by further experimental studies. Diffusion coefficients for low porosities in salt grit are not well known. The diffusion coefficient of $1 \cdot 10^{-10}$ m^2/s seems to be far too high. The total release of the radionuclides from the canisters into a small saturated void volume within a short period of time may be overly pessimistic and not realistic. For all radionuclides with unknown solubility limit total dissolution in brine is assumed. All these assumptions should be investigated in future R&D work.

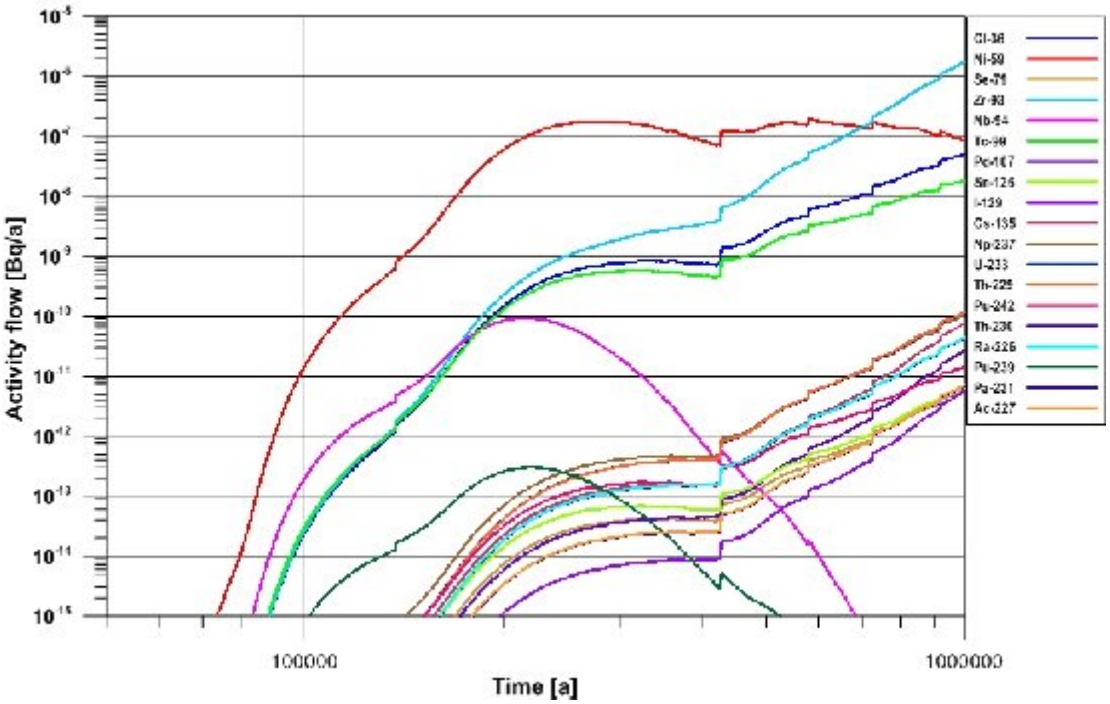

Fig. 5. Evolution of the activity flow of some important radionuclides. Expected lifetime for the shaft seals 50,000 a, final porosity 2 %, diffusion-coefficient of $1 \cdot 10^{-10}$ m^2/s.

Results of TOUGH2 Calculations

In an accompanying paper [21] and also in [22] it was shown that the integrity of the host rock is not threatened by thermo-mechanical processes induced by the heat-generating waste. Extremely high gas pressure, therefore, may become important when considering the integrity of the rock salt.

For several simulation cases (P1 to P8), maximum pressures were calculated (see Fig. 6). In most cases, maximum pressure rose to approx. 16 MPa for model runs with a final porosity of 1 %. Only one model run (P-2) showed significantly higher pressures, which exceeded 18.8 MPa (lithostatic pressure). These pressures were calculated exclusively in the southern emplacement drift of field East 12. The main reason for the high pressure was the slow corrosion. After 100 years, compaction was finished but the corrosion process continued up to 5000 years for a corrosion rate of 0.1 □m/a. For an even slower corrosion, however, pressures did not reach lithostatic pressures.

The reason is that gas generation rate in this case was exceeded by the capability of the gas to flow out of the emplacement drift. This was possible despite the low porosity and permeability. This is because limited gas advection with very low magnitudes is always possible (see Eq. 2 and Table II) in these calculations. The long-term hydraulic behavior of the repository system is governed by this assumption.

For this reason further R&D work regarding the characterization of two-phase behavior of salt grit at very low porosities is required.

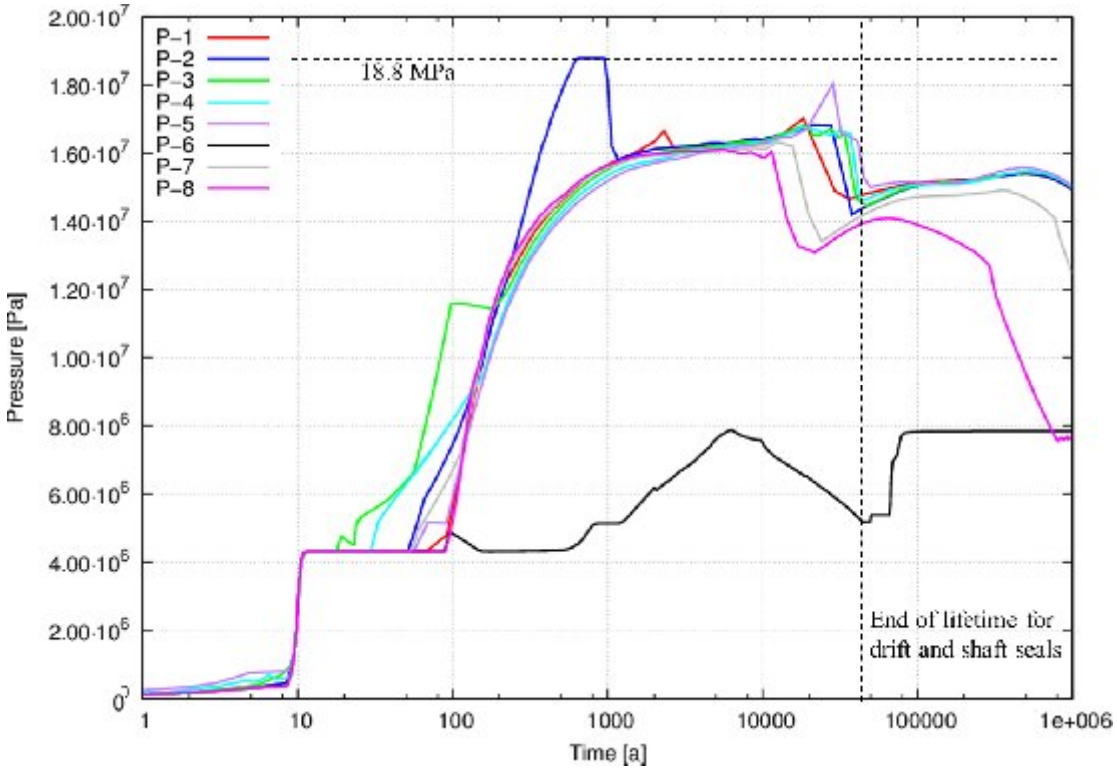

Fig. 6. Evolution of maximum calculated gas pressure anywhere the repository. Lithostatic pressure was 18.8 MPa, end of lifetime for barriers 50,000 years (dashed lines).

After 10,000 years, when no more gas is generated by corrosion, maximum pressures drop about 2 MPa. After a slight increase coinciding with the end of drift seal lifetime at 50,000 years, the graphs show that maximum pressures slowly decreased again. The reason for this is that continuing advection in the repository lead to gas pressure equilibrium.

The characteristic of the maximum pressure curve depended on final porosity. At a slightly higher final porosity (and thus permeability) gas pressure equilibrium was reached earlier (slightly less than 8 MPa, case P-6). It is likely that for the other cases (P-1 to P-5) the pressure equilibrium would be higher. A drop

of porosity from 2 % to 1 % reduces available pore space by a factor of 2 in all emplacement fields. Final gas pressure therefore would likely to double to approx. 16 MPa and at a later time. However, the graphs show final pressures tending more to 15 MPa than to 16 MPa. This is because at 1 % porosity and very low permeability gas was still flowing into the local sink, the infrastructure area.

Regarding cases P-7 and P-8 less gas was generated and additional pore space was available for gas (P-8). That means that equilibrium pressure in the repository was lower, which can be seen for case P-8.

Gas pressures in consequence lead to gas transport. In Fig. 7a and 7b show flow of gas and radionuclide (C-14) through the drift seals. The amount of released radionuclides was very small compared to the amount of water and gas in the repository.

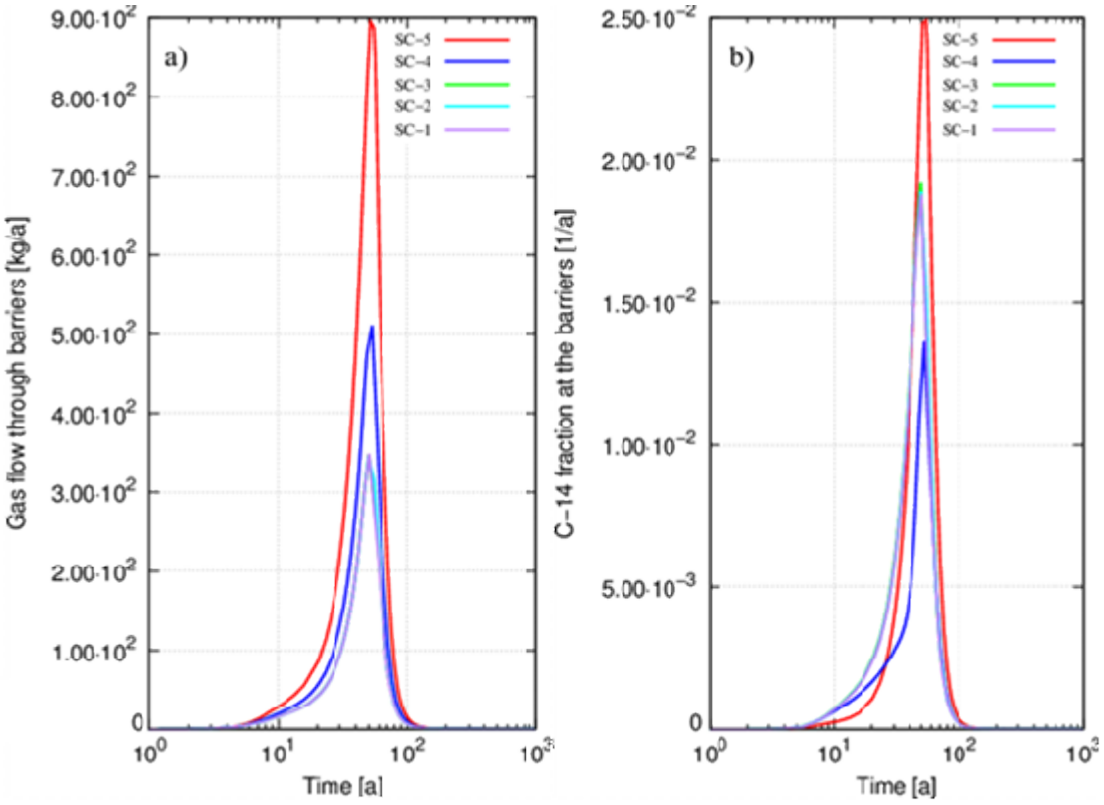

Fig. 7. a) Total gas flow through both drift seals. b) Evolution of total volatile C-14 flow through both drift seals (normalized to total C-14 release from structural components).

As shown in Fig. 7a magnitude of gas flow through the barriers depended to a certain extent on the rate of corrosion [22]. In contrast, significant gas flow through the drift seals was also computed in case SC-1, where no corrosion occurred. This indicates that the calculated magnitude of gas flow in case SC-1 corresponds to a baseline value for gas flow through the drift seals. This shows that the compaction of the salt grit is likely to be the main driving force for most of the initial gas flow through the drift seals. Only the incremental increase of gas flow magnitude between cases SC-1 through SC-5 is caused by increase of corrosion rates. Maximum gas flow was calculated for case SC-5 with the highest corrosion rate.

Significant gas flow out of the repository raises the question if radionuclides are transported within the gas by advection. To that regard, Fig. 7b shows the flow of C-14 through both drift seals for cases SC-1 to SC-5. A significant fraction of the released C-14 tracer is transported through the drift seals per year.

Maximum release rates for case SC-5 amount to 2.5 % per year of initially released C-14. After 100 years approx. 23.4 % of the initially released radionuclides have been transported through the drift seals, after 1000 years only 0.2 % more (23.6 %). For longer times, these relations get meaningless since half-life of C-14 was taken into account (5730 a). At first glance, C-14 release and total gas flow magnitude correlate very well. In fact, this is not the case. Calculation cases with lowest gas flow show consistently show medium C-14 release (SC-1 to SC-3). Interestingly, case SC-4 showed lowest C-14 release but medium gas flow. Additional differences in C-14 transport through the drift seals can be seen at the slope of the curves. Therefore transport of gas was independent of the release of radionuclides.

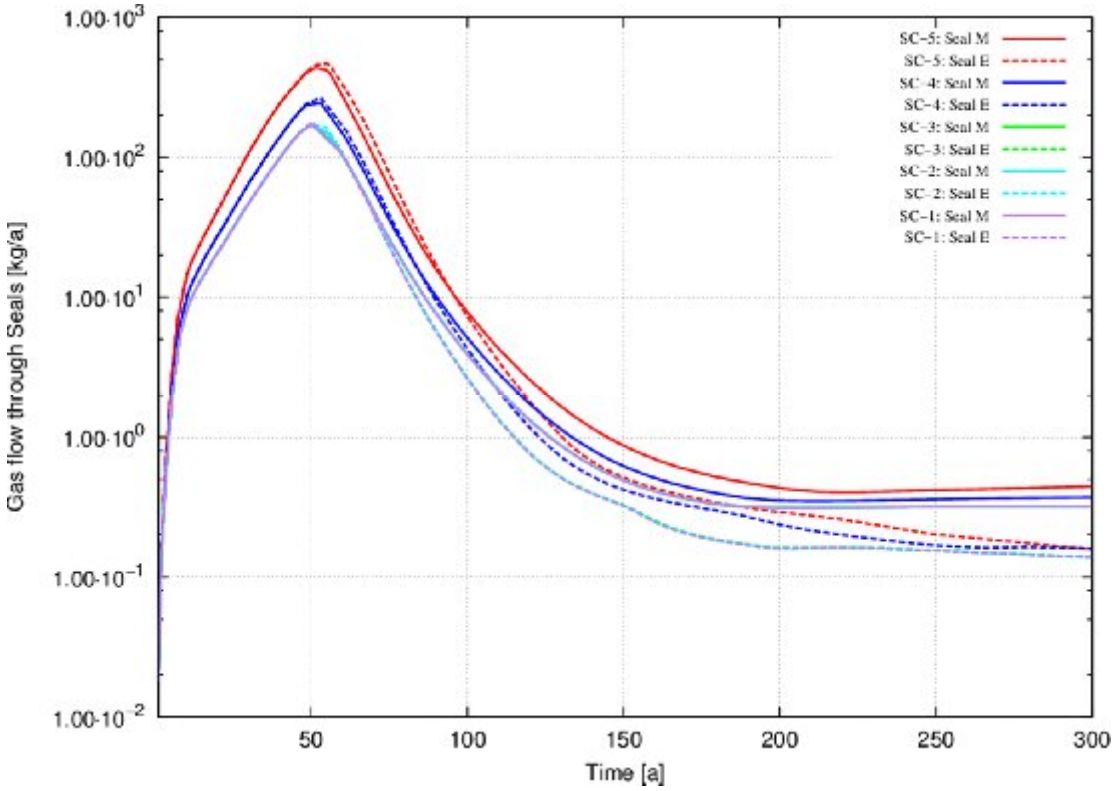

Fig. 8. Gas flow through each drift seal. Seal locations for “E” and “M” are shown in Fig. 3.

There may be many reasons for these differences but two obvious ones come to mind. The first may be that the total gas flow through the drift seals (Fig. 7a) was dominated by only one drift seal. That would mean that C-14 could 'stay' on one side of the drift seal but is not transported through it. The second possibility is that C-14 is transported in a different way right from the start when it is released in the emplacement drift. The first reason is unlikely as the modeled gas flow through each drift seal is similar for each model case: This is illustrated in Fig. 8 gas flow for the respective drift seals show that in each model case gas flow through each drift seal occurred. Examination of the latter point requires more detailed analyses of flow paths inside the repository.

One additional interesting observation, which cannot be shown in any of these figures, is that no radionuclide flow (or 'leakage') through the shaft seals out of the mine occurs.

CONCLUSIONS

For the described *B1*-concept, transport of radionuclides via the liquid phase was calculated with the code MARNIE. In the numerical cases with 1 % final porosity no release of radionuclides can be observed. Even when the shaft seals are postulated to be dysfunctional directly after repository closure, no brine inflow can be found, since the salt grit in the main drifts already reached the final porosity of 1 %.

Transport of radionuclides only occurs for a final porosity of 2 % when advective flow and diffusive transport of radionuclides are assumed. At the end of the simulation time after 10^6 years a large number of emplacement fields were saturated with brine. Due to the fact that some areas remain unsaturated, the pressure driven inflow over the shafts continues to take place. Consequently the outflow of radionuclides towards the drift seals was only driven by diffusion. The radionuclides with the highest activity flow at the eastern drift seal were Ni-59, Zr-93, Tc-99 and Cl-36. All other radionuclides considered show an increase in activity flow, but with a lower maximum.

Many assumptions for the preliminary MARNIE and TOUGH2 calculations are very conservative and should be investigated in future R&D work. The main ones are:

i) the possibility of advective and diffusive transport of radionuclides at low salt grit porosities (≤ 1% for TOUGH2 calculations),
ii) the diffusion coefficient in high compacted salt grit of $1 \cdot 10^{-10}$ m^2/s,
iii) the unknown solubility limits for some radionuclides and
iv) the fast release of radionuclides into a small void volume.

In contrast, transport of radionuclides via the gas phase leads to a significant flow of C-14 through both drift seals into the infrastructure area soon after repository closure – regardless of final porosity. There are mainly two reasons for this.

First of all, the physical processes lead to a great amount of gas flow (air) out of the repository in the few decades following closure. Gas generation – especially early after closure due to high corrosion rates – amplifies gas flow through the drift seals. Predominantly however, it seems that salt grit compaction is the main driving force for gas flow.

Secondly, structural components from the decommissioning of fuel rods were emplaced very close to a drift seal ("Seal E") leading to a relatively high amount of transported radionuclides. In addition, the infrastructure area lying outside the CPRZ had been designed as a sink for fluids in the first place.

For both reasons optimizing strategies regarding the repository design are conceivable. A repository layout where the structural components were emplaced farther away from the drift seals would likely yield different results with less C-14 flow through the drift seals. Furthermore, implementing a sink (like the infrastructure area) enclosed in the CPRZ might inhibit gas flow through the drift seals. Also, it may be possible to use (initially) gas tight casks for the structural components (e.g. Pollux®) to contain volatile radionuclides over a longer period.

REFERENCES

1. Bracke, G., K. Fischer-Appelt, and B. Baltes. *Overview on the Preliminary Safety Analysis of the Gorleben Site - 13298*, in *WM2013*. 2013, Phoenix,
2. Bundesministerium für Umwelt, Naturschutz und Reaktorsicherheit (BMU), *Safety Requirements Governing the Final Disposal of Heat-Generating Radioactive Waste*, 2010, Bonn, Germany.

3. Bollingerfehr, W., et al., *Endlagerkonzepte*, 2011, Gesellschaft für Anlagen- und Reaktorsicherheit (GRS) mbH, Köln.
4. Bollingerfehr, W., et al., *Endlagerauslegung und -optimierung*, 2012, Gesellschaft für Anlagen- und Reaktorsicherheit (GRS) mbH, Köln.
5. Czaikowski, O. and K. Wieczorek, *Salzgruskompaktion – Kalibrierung der in CODE_BRIGHT verwendeten physikalischen Modellansätze zur numerischen Simulation*, 2012, Gesellschaft für Anlagen- und Reaktorsicherheit (GRS) mbH, Braunschweig.
6. Müller-Hoeppe, N., et al., *Integrität geotechnischer Barrieren – Teil 1: Vorbemessung*, 2012, Gesellschaft für Anlagen- und Reaktorsicherheit (GRS) mbH, Köln.
7. Müller-Hoeppe, N., et al., *Integrität geotechnischer Barrieren – Teil 2: Vertiefte Nachweisführung*, 2012, Gesellschaft für Anlagen- und Reaktorsicherheit (GRS) mbH, Köln.
8. Pruess, K., C. Oldeburg, and G. Moridis, *TOUGH2 User's Guide*, 1999, Earth Sciences Division, Lawrence Berkeley National Laboratory, University of California, Berkeley, California 94720.
9. Martens, K.-H., H. Fischer, and P. Romstedt, *Beschreibung des Rechenprogrammes MARNIE*, 2002, Gesellschaft für Anlagen- und Reaktorsicherheit (GRS) mbH, Köln.
10. Becker, A., et al., *Evaluation of elements responible for the effective engaged dose rates associated with the final storage of radioactive waste: EVEREST project*, 1997, Eurpean Commission, Luxembourg, 92-828-0531-X.
11. CODE-BRIGHT, *A 3-D program for thermo-hydro-mechanical analysis in geological media*, 2002, Universidad Politécnica de Cataluña (UPC),
12. Kröhn, K.-P., et al., *Restporosität und -permeabilität von kompaktierendem Salzgrus-Versatz REPOPERM - Phase 1*, 2009,
13. Larue, J., et al., *Radiologische Konsequenzenanalyse*, 2012, Gesellschaft für Anlagen- und Reaktorsicherheit (GRS) mbH, Köln.
14. Kock, I., et al., *Integrität des einschlusswirksamen Gebirgsbereiches - Systemanalyse und Systemverständnis, Bericht für Arbeitspaket 9a im Vorhaben „Vorläufige Sicherheitsanalyse für den Standort Gorleben"*, 2011,
15. Dörr, S., Bollingerfehr, W., Filbert W., Tholen M., *In das Endlager eingebrachte Inventare an Metallen, Organika und weiteren Stoffen. Memo im Arbeitspacket 5, Vorläufige Sicherheitsanalyse für den Standort Gorleben* 2012, DBE-TEC, Peine.
16. Peiffer, F., et al., *Abfallspezifikation und Mengengerüst. Basis Ausstieg aus der Kernenergienutzung (Juli 2011)*, 2011, Gesellschaft für Anlagen- und Reaktorsicherheit (GRS) mbH, Köln.
17. Mönig, H., *Literaturstudie zur Metallkorrosion im Rahmen der „Vorläufigen Sicherheitsanalyse Gorleben"*, 2011, Gesellschaft für Anlagen- und Reaktorsicherheit (GRS) mbH, Braunschweig.
18. Kienzler, B., et al., *Radionuclide Source Term for HLW Glass, Spent Nuclear Fuel, and Compacted Hulls and End Pieces (CSD-C Waste)*, 2012, Karlsruher Institut für Technologie - Institut für Nukleare Entsorgung (KIT-INE), Karlsruhe.
19. Sander, R. *Henry's Law Constants*. NIST Chemistry WebBook, NIST Standard Reference Database Number 69, 1999, cited 2012 9/27; Available from: http://webbook.nist.gov.
20. Kienzler, B., et al., *Source Term for Irradiated Fuel from Prototype, Research and Education Reactors, for Non Heat Producing Waste Forms and for Uranium Tails*, 2012, Karlsruher Institut für Technologie - Institut für Nukleare Entsorgung (KIT-INE), Karlsruhe.
21. Eickemeier, R., et al. *Preliminary Safety Analysis of the Gorleben Site: Thermo-mechanical Analysis of the Integrity of the Geological Barrier in the Gorleben Salt Formation - 13307*, in *WM2013*. 2013, Phoenix,
22. Kock, I., et al., *Integritätsanalyse der geologischen Barriere*, 2012, Gesellschaft für Anlagen- und Reaktorsicherheit (GRS) mbH, Köln.